

# Spontaneous behavior and magnetic field and pressure effects on $\text{La}_{2/3}\text{Ca}_{1/3}\text{MnO}_3$ perovskite

J. M. De Teresa, M. R. Ibarra, J. Blasco, J. García, C. Marquina, and P. A. Algarabel

*Departamento de Física de la Materia Condensada and Instituto de Ciencia de Materiales de Aragón, Universidad de Zaragoza and Consejo Superior de Investigaciones Científicas, 50009, Zaragoza, Spain*

Z. Arnold and K. Kamenev

*Institute of Physics, Academy of Sciences of Czech Republic, Cukrovarnická 10, 162 00 Praha 6, Czech Republic*

C. Ritter

*Institut Laue-Langevin, Boîte Postale 156, 38042 Grenoble Cédex 9, France*

R. von Helmolt

*Siemens AG, Research Laboratories, D-8520 Erlangen, Germany*

(Received 15 January 1996)

The effects of magnetic field and pressure on the unusual spontaneous behavior of  $\text{La}_{2/3}\text{Ca}_{1/3}\text{MnO}_3$  have been thoroughly investigated. Resistivity and volume thermal expansion, both under magnetic field and pressure, ac susceptibility under pressure, magnetostriction, magnetoresistance, and neutron diffraction measurements, have allowed us to determine the relevant underlying mechanisms in this system. Above  $T_c$  the neutron measurements reveal short-range ferromagnetic correlations and the anomalous volume thermal expansion indicates that local distortions are present. Both experiments support the formation of magnetic polarons above  $T_c$ . At  $T_c$  the compound undergoes a paramagnetic-ferromagnetic transition accompanied by an insulator-metal-like transition with anomalies in the electrical and volume properties. Above  $T_c$  the magnetic field and the pressure favor electrical conduction by enhancing the double-exchange interaction. Below  $T_c$  the metallic state is favored by the magnetic field and the pressure in a different way. [S0163-1829(96)04726-1]

## I. INTRODUCTION

Given that  $\text{La}_{2/3}\text{Ca}_{1/3}\text{MnO}_3$  (and related compounds) could be used as a magnetoresistive material, a careful and complete study of its magnetic, transport, and structural properties is warranted. We need to take into account the behavior under magnetic field and pressure to build a coherent picture of this system. Consequently, we have carried out measurements of resistivity and volume thermal expansion, both under magnetic field and pressure, ac susceptibility under pressure, magnetoresistance, magnetostriction, and neutron diffraction measurements. In Sec. II we describe the experimental techniques we have used, and in Sec. III we report the obtained results along with the theory which supports them.

The series  $\text{La}_{1-x}\text{Ca}_x\text{MnO}_3$  was first studied by Jonker and Van Santen in the 1950s.<sup>1</sup> For  $x \geq 0.15$  the compounds show a pseudocubic perovskitelike structure. In this structure, if we take the La(Ca) ions at the origin of the unit cell, the Mn ions occupy the corners of the cube and surrounding each Mn ion there are six  $\text{O}^{2-}$  ions forming an octahedron. At and around  $x=1/3$ , the compounds order ferromagnetically. Zener<sup>2</sup> proposed the double-exchange (DE) interaction as the mechanism responsible for the alignment of the Mn magnetic moments. Substitution of a trivalent ion ( $\text{La}^{3+}$ ) by a divalent ion ( $\text{Ca}^{2+}$ ) causes coexistence of  $\text{Mn}^{3+}$  and  $\text{Mn}^{4+}$  ions in the appropriate ratio. The DE interaction consists of the transfer of the ‘‘extra’’ electron between neighboring Mn ions through the  $\text{O}^{2-}$  ions, which results in an effective ferromagnetic interaction due to the strong on-site Hund’s cou-

pling. The Mn spin alone accounts for the experimental saturation magnetization of  $\text{La}_{2/3}\text{Ca}_{1/3}\text{MnO}_3$ .<sup>1,3</sup> The electrical conductivity of  $\text{La}_{2/3}\text{A}_{1/3}\text{MnO}_3$  ( $\text{A}=\text{Ca},\text{Sr},\text{Ba}$ ) compounds was found to be unusual:<sup>4</sup> It behaves semiconductorlike above  $T_c$  and metalliclike below  $T_c$ .

The renewed interest in  $\text{La}_{2/3}\text{Ca}_{1/3}\text{MnO}_3$  and related compounds arose after the discovery of giant magnetoresistance (GMR) at and around  $T_c$ .<sup>5-9</sup> Recently, colossal magnetoresistance ratios have been observed in related compounds at low temperatures.<sup>10,11</sup> The challenge is to achieve such colossal magnetoresistance ratios at room temperature. Meanwhile, interest in  $\text{La}_{2/3}\text{Ca}_{1/3}\text{MnO}_3$  continues as it shows GMR ratios near room temperature.

It is widely accepted that the ferromagnetic transition in  $\text{La}_{2/3}\text{Ca}_{1/3}\text{MnO}_3$  (and related compounds) is simultaneous with an insulator-metal transition.<sup>12,13</sup> The mechanism which drives the transition is still uncertain. The DE interaction alone cannot account for the resistance curves.<sup>14</sup> Some theoretical works<sup>15-18</sup> have tried to explain the GMR ratios using different approaches. Experimentally, Hwang *et al.*<sup>12</sup> have shown important lattice effects in doped  $\text{LaMnO}_3$  and Ibarra *et al.*<sup>19</sup> have found strong lattice distortions and magnetoelastic coupling in Y-doped  $\text{La}_{2/3}\text{Ca}_{1/3}\text{MnO}_3$ , which was subsequently confirmed by spectroscopy experiments.<sup>20</sup>

It is important to notice that the GMR ratios and the  $T_c$  values of  $\text{La}_{2/3}\text{Ca}_{1/3}\text{MnO}_3$  (and related compounds) reported by different authors can differ remarkably depending on the author. Thin films and polycrystals usually have different  $T_c$  values and consequently different magnetoresistance values.  $T_c$  varies with oxygen content<sup>21</sup> and  $\text{Ca}^{2+}$

concentration,<sup>1</sup> and the resistance depends on the grain size.<sup>22</sup> Diffusion is also an important factor which depends on the heat treatment.<sup>23</sup> Nevertheless, the overall behavior is identical for all samples.

## II. EXPERIMENTS

Two different polycrystalline samples were used for the experiments. One of the samples (called sample 1 hereafter) was used for all the experiments except for the neutron diffraction measurements. Sample 1 was produced at the Siemens Laboratory. It was prepared by repeated grinding and annealing from the metal carbonates and oxides. Then it was cold pressed and annealed in air at 1450 °C for 30 h (slow heating and cooling). The second sample was prepared at the University of Zaragoza (called sample 2 hereafter) and was used for the neutron diffraction measurements. This sample was tested to have similar bulk thermal, electrical, and magnetic properties as sample 1. Sample 2 was prepared using a gel precursor in order to obtain well-mixed reagents. Stochiometric amounts of La<sub>2</sub>O<sub>3</sub>, CaCO<sub>3</sub>, and MnCO<sub>3</sub> with nominal purities higher than 99.9% were dissolved in concentrated nitric acid, resulting in a light solution. Afterwards, citric acid and ethylene glycol were added in a ratio of 4 g citric acid to 1 ml ethylene glycol and 1 g metal nitrates. The solution was heated and the excess nitric acid and water were boiled off, giving a yellow-brown gel. The gel was heated to give a brown powder. This precursor was calcined at 1173 K overnight. The remaining black powder was cold pressed to 4 kbar and sintered at 1273 K for 3 days with intermediate grindings. Finally, the pellet was sintered at 1573 K for 8 h, resulting in a hard black ceramic material. Energy dispersive x-ray (EDAX) analysis was performed over the two samples by using scanning electron microscopy. The obtained atomic ratio was La:Ca:Mn=0.72:0.28:1 (±0.01) for sample 1 and La:Ca:Mn=0.68:0.32:1 (±0.01) for sample 2. These results show a slight deviation from nominal composition for sample 1. Step-scanned x-ray diffraction patterns were carried out from 18° to 140° in 2 $\theta$  with a step of 0.02°. Full profile analysis was performed by using the Fullprof program. The La/Ca ratio was refined resulting the values La:Ca:Mn=0.74:0.26:1 (±0.02) for sample 1 and La:Ca:Mn=0.66:0.34:1 (±0.02) for sample 2, in good agreement with EDAX analysis. The room-temperature lattice parameters were found to be  $a=5.4831(4)$ ,  $b=5.4706(4)$ , and  $c=7.7283(6)$  for sample 1 and  $a=5.4717(2)$ ,  $b=5.4569(2)$ , and  $c=7.7112(3)$  for sample 2. Sample 1 shows a higher unit cell volume due to the higher La/Ca ratio. The oxygen content was analyzed by redox titration. The resulting chemical formulas were La<sub>0.72</sub>Ca<sub>0.28</sub>MnO<sub>2.96±0.02</sub> for sample 1 and La<sub>0.68</sub>Ca<sub>0.32</sub>MnO<sub>2.98±0.02</sub> for sample 2.

Above room temperature the volume thermal expansion was measured with a ‘‘push rod’’ and differential-transformer method. Below room temperature resistance (magnetoresistance) and volume thermal expansion under magnetic field were measured in a superconducting coil which produces steady magnetic fields up to 12 T. The resistance was measured with the four-point technique and the volume thermal expansion with the strain-gauge technique. Resistance and volume thermal expansion under pressure were measured with the same techniques, the pressure being

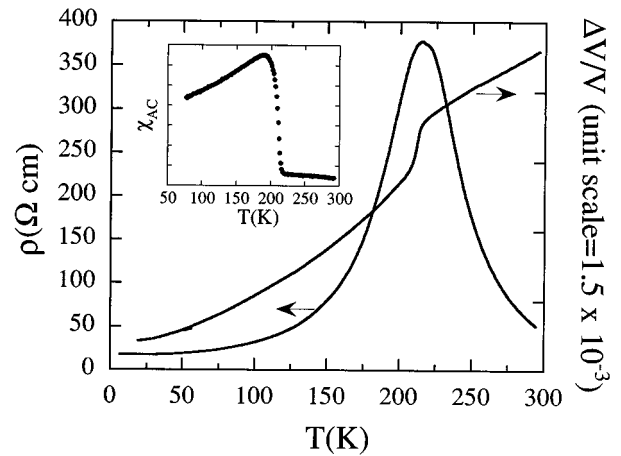


FIG. 1. Spontaneous resistivity ( $\rho$ ) and volume thermal expansion ( $\Delta V/V$ ) as a function of temperature. The inset shows the ac susceptibility ( $\chi_{ac}$ ) vs  $T$ .

produced by a CuBe cell which attains hydrostatic pressures up to 9 kbar. Pressure and temperature were measured *in situ* using a manganin pressure sensor and a Thermocoax thermocouple, respectively. The same cell was used for the ac susceptibility under pressure measurements. In our setup the sample formed the core of a microtransformer with four turns in both primary and secondary coils. Magnetostriction up to 14.2 T was measured in a pulsed-field device using the strain-gauge technique. The strain parallel ( $\lambda_{\parallel}$ ) and perpendicular ( $\lambda_{\perp}$ ) to the applied field was measured. Volume magnetostriction ( $\omega$ ) and anisotropic magnetostriction ( $\lambda_t$ ) are straightforwardly calculated as  $\omega = \lambda_{\parallel} + 2\lambda_{\perp}$  and  $\lambda_t = \lambda_{\parallel} - \lambda_{\perp}$ , respectively. The neutron diffraction experiments were performed using the D1B high-intensity powder diffractometer at the Institut Laue-Langevin (ILL), Grenoble, using a wavelength of 2.52 Å. D1B has a 400-element linear multidetector, covering an angular range of 80°. The powdered sample was placed in a standard ILL cryofurnace. Diffraction patterns were collected between 2 $\theta=2.5^\circ$  and 82.5° at temperatures ranging from 1.5 to 540 K.

## III. RESULTS AND DISCUSSION

### A. Spontaneous behavior

In Fig. 1 the spontaneous behavior of resistivity, thermal expansion, and ac susceptibility of the sample below room temperature is shown. At  $T \approx 215$  K a ferromagnetic transition takes place and the ac susceptibility (see inset of Fig. 1) displays a sharp increase.  $T_c \approx 215$  K for sample 1 is lower than other values found in polycrystals of similar composition (our sample 2 or those mentioned in Ref. 24). The different methods of preparation gave different Ca<sup>2+</sup> concentrations (as explained in the previous section), which is at the origin of this discrepancy. The existence of long-range ferromagnetic order in this kind of compound was explained with the DE interaction.<sup>3</sup> In La<sub>2/3</sub>Ca<sub>1/3</sub>MnO<sub>3</sub> the Mn<sup>4+</sup> ions have three  $d$  electrons, with  $t_{2g}$  symmetry, which are localized at the Mn sites. Along with these  $t_{2g}$  electrons, the Mn<sup>3+</sup> ions have a fourth electron, an  $e_g$  electron, which is not localized and can be transferred between adjacent Mn

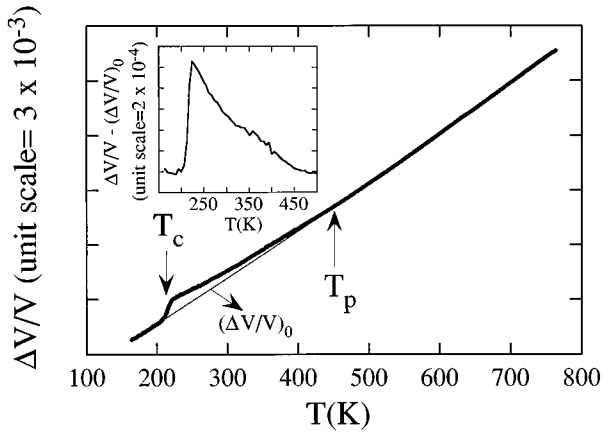


FIG. 2. High-temperature volume thermal expansion ( $\Delta V/V$ ) and simulated phonon contribution  $(\Delta V/V)_0$ . The inset shows in detail the anomalous contribution over the phonon contribution.

ions through the path Mn-O-Mn. Because of the strong on-site Hund's coupling, at a Mn site the  $t_{2g}$  and  $e_g$  electrons have parallel spins. When the  $e_g$  electron moves from one Mn site to another Mn site, it keeps its spin direction and couples with the corresponding  $t_{2g}$  electrons. Then an effective ferromagnetic interaction between neighboring Mn spins arises. The DE interaction has to compete with the antiferromagnetic superexchange (AS) interaction, and consequently different magnetic structures or even the absence of long-range order can take place.<sup>3,24,25</sup> In  $\text{La}_{2/3}\text{Ca}_{1/3}\text{MnO}_3$  the DE interaction overcomes the AS interaction and long-range ferromagnetic order occurs.

Cooling down from room temperature, the resistivity increases tremendously down to  $T_c$  (see Fig. 1). The mechanism which produces such unusual increase is of great interest. Kusters *et al.*<sup>5</sup> proposed conduction by magnetic polarons above  $T_c$  as in magnetic semiconductors. This assumption was supported by fits of resistivity curves above  $T_c$  with exponential laws, which can be a signal of conduction by thermal hopping.<sup>26</sup> This idea was widely accepted, but no clear evidence of the existence of magnetic polarons was given.<sup>27</sup> A magnetic polaron consists of an electron (or a wave packet of electrons<sup>18</sup>) which becomes localized, polarizing the spins around it. Then a magnetic cluster forms. According to Coey *et al.*<sup>18</sup> it is unlikely that these polarons can diffuse as a whole. Instead, individual electrons will hop between neighboring clusters. Ibarra *et al.*<sup>19</sup> have given evidence for charge localization accompanied by lattice distortion above  $T_c$  in Y-doped  $\text{La}_{2/3}\text{Ca}_{1/3}\text{MnO}_3$ . In Fig. 2 we can see that the same effect takes place in pure  $\text{La}_{2/3}\text{Ca}_{1/3}\text{MnO}_3$ . Cooling down from high temperature, an extra contribution appears below  $T_p$  over the anharmonic phonon contribution in the volume thermal expansion. This extra contribution rapidly vanishes at  $T_c$ . This anomalous effect is thought to be caused by the gradual charge (the  $e_g$  electrons) localization below  $T_p$ , which causes lattice distortions. These seem to be dynamic Jahn-Teller-like distortions.<sup>20</sup> If an electron which becomes localized polarizes the spin of the neighboring ions, then a magnetic polaron would form. These magnetic clusters would give an extra contribution to the small-angle neutron scattering (SANS). For instance, magnetic clusters around  $T_c$  enhance the SANS, which is commonly known as

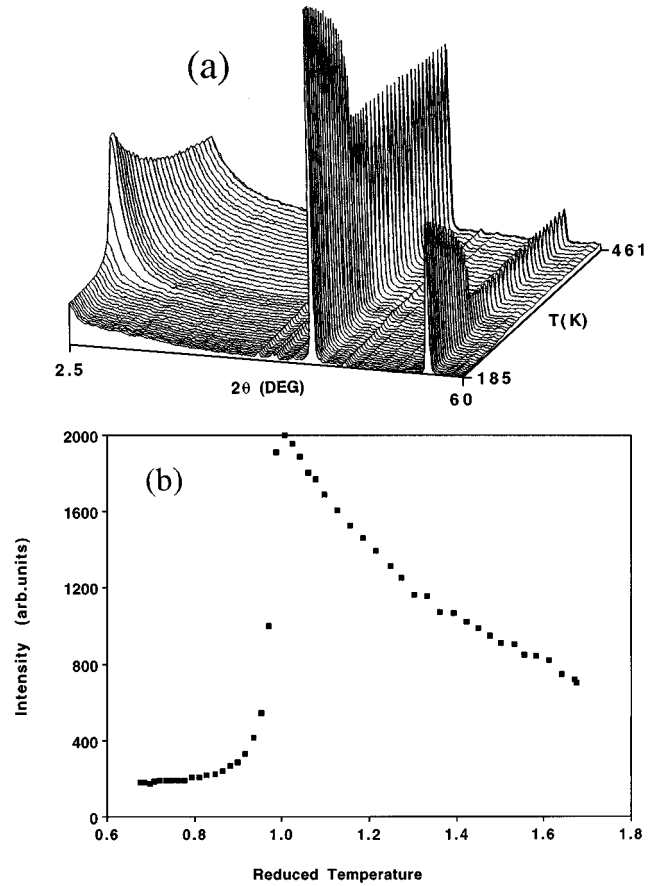


FIG. 3. (a) Neutron diffraction pattern at temperatures ranging from 185 to 461 K and at angles between  $2\Theta=2.5$  and  $60^\circ$ . (b) The SANS intensity in arbitrary units at  $2\Theta=2.5^\circ$  as a function of the reduced temperature  $T/T_c$ .

“critical scattering.”<sup>28</sup> The critical scattering of  $\alpha$ -Fe is an archetypal example of this effect.<sup>29</sup> In Figs. 3(a) and 3(b) we can observe the SANS ( $2.5^\circ$ ) of  $\text{La}_{2/3}\text{Ca}_{1/3}\text{MnO}_3$  in a wide range of temperatures. The result is intriguing. Unlike the  $\alpha$ -Fe SANS pattern, the  $\text{La}_{2/3}\text{Ca}_{1/3}\text{MnO}_3$  SANS scattering is not roughly symmetric around  $T_c$  and it exists far above  $T_c$ . This result seems to indicate that magnetic clusters (short-range magnetic order) exist far above  $T_c$  in the paramagnetic region. Therefore the volume thermal expansion and the SANS results support the formation of magnetic polarons above  $T_c$ . A more detailed analysis of the SANS results in order to get information about the magnetic correlation length and, consequently, the cluster size was not successful because of the experimental limitation of the D1B instrument. A more in-depth study of this magnitude would require an instrument more appropriate for SANS measurements.

At  $T_c$ , when the long-range magnetic order sets in, a magnetic contribution appears on the nuclear peaks below  $T_c$  [see Fig. 3(a)] and simultaneously a sharp lattice contraction takes place ( $\approx 0.1\%$ ) (see Figs. 1 and 2). Ibarra *et al.*<sup>19</sup> have interpreted this result as the delocalization of the  $e_g$  electrons which had become localized in the paramagnetic regime. Then the extra contribution over the phonon one to the volume thermal expansion disappears (see Fig. 2). Below  $T_c$  the resistivity curve shows metallic behavior. It can be explained

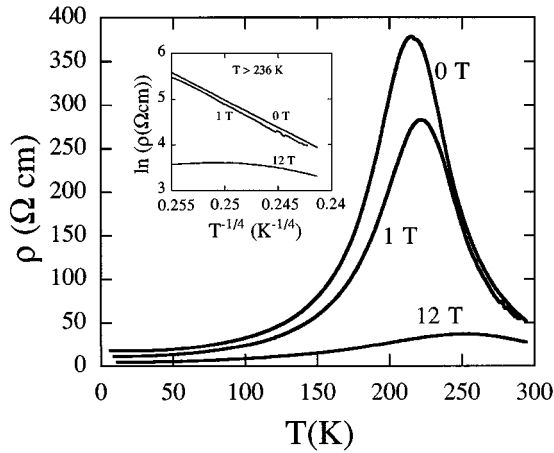


FIG. 4. Resistivity ( $\rho$ ) as a function of temperature at magnetic field values of 0, 1, and 12 T. The inset shows  $\ln \rho$  vs  $T^{-1/4}$  at temperatures above  $T_c$ .

as follows. The conduction takes place via the  $e_g$  electrons. According to de Gennes<sup>30</sup> the transfer of an  $e_g$  electron between two Mn ions is proportional to  $\cos(\Theta_{ij}/2)$ , where  $\Theta_{ij}$  is the angle between the two ionic spins. As  $T$  is lowered,  $\Theta_{ij}$  will decrease owing to the ferromagnetic alignment of the Mn spins and consequently  $\rho$  will decrease too.

### B. Effect of magnetic field

The effect which triggered the interest of the scientific community in this kind of compound was the exhibition of GMR. We can observe in Fig. 4 the curves of  $\rho$  vs  $T$  under magnetic fields of 0, 1, and 12 T. The magnetic field reduces the localization process remarkably, and the insulator-metal transition becomes smoother, almost missing. In order to check if above  $T_c$  the resistivity can be fit to the Mott's law  $\rho = \exp(T_0/T^{1/4})$ , which corresponds to a model of variable-range hopping of electrons in a band of localized states in the absence of electron-electron interactions, we have plotted  $\ln \rho$  vs  $T^{-1/4}$  in the inset of Fig. 4. Under 0 and 1 T the curves display a linear form, which is in agreement with conduction by polarons.<sup>18</sup> The way the magnetic field affects the transfer of electrons between neighboring Mn sites (or, equivalently, the delocalization of the  $e_g$  electrons) is easily understood if we take into account that such transfer can be expressed as  $t_{\text{eff}} = t_0 \cos(\Theta/2)$ , where  $t_0$  depends on geometric structural parameters (essentially the angle and length of the Mn-O bond) and  $\Theta$  is the angle between neighboring Mn spins. The magnetic field will align the spins and  $\Theta$  will decrease,  $t_{\text{eff}}$  being enhanced. As the electron is delocalized now, the polaron will not form.

The mechanism of conduction below  $T_c$  is a subject of interest as well. Schiffer *et al.*<sup>24</sup> analyzed the low-temperature resistivity curves of  $\text{La}_{0.75}\text{Ca}_{0.25}\text{MnO}_3$  and found for  $T < 0.5T_c$  the empirical expression  $\rho(T) = \rho_0 + \rho_1 T^{2.5}$ . The term  $\rho_0$  is the resistivity due to domain and grain boundaries and other temperature-independent scattering mechanisms [presumably defects (mainly chemical, nonstoichiometry, etc.)], and the  $\rho_1 T^{2.5}$  term is an empirical fit to the data which represents a combination of electron-electron, electron-phonon, and electron-magnon scattering, all of

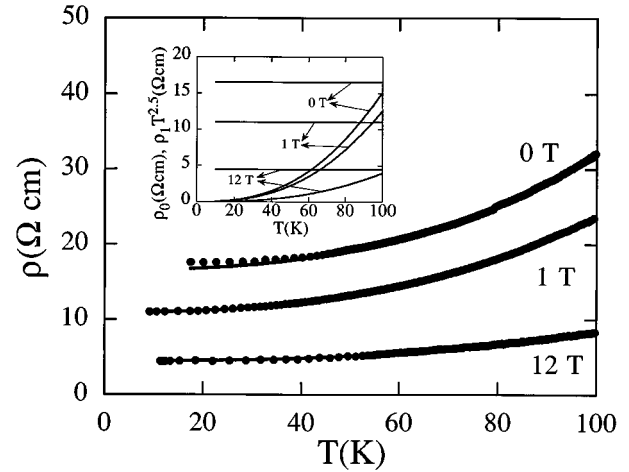


FIG. 5. Fits of the low-temperature resistivity to the expression  $\rho(T) = \rho_0 + \rho_1 T^{2.5}$ . The inset shows the contributions  $\rho_0$  and  $\rho_1 T^{2.5}$  to the resistivity as a function of temperature.

which are expected to be significant in this system.<sup>24</sup> We have tried to fit our low-temperature results with different exponents for the term  $\rho_1 T^\nu$  and  $\nu \approx 2.5$  was also found to give the best fit for all the magnetic fields. In Fig. 5 we show the fits to our experimental data, and in the inset of Fig. 5 we have plotted the contribution of the two terms  $\rho_0$  and  $\rho_1 T^{2.5}$  as a function of temperature. From there we can extract information of how the magnetic field affects the mechanism of conduction. A field of 1 T strongly affects the temperature-independent term  $\rho_0$ , whereas it has less influence on the temperature-dependent term  $\rho_1 T^{2.5}$ . It is likely that the main mechanism responsible for the magnetoresistance at low temperatures and low fields is the influence of the magnetic field on the magnetic domains. As low magnetic fields increase the size of the magnetic domains, the scattering of the electrons due to domain boundaries decreases and the magnetization becomes larger.<sup>22,24</sup> Fields greater than 1 T seem to affect both mechanisms (the temperature-dependent and the temperature-independent scattering) to a similar degree.

The anomalous spontaneous volume thermal expansion was linked to the local distortion caused by the localization of the  $e_g$  electrons. If this localization process is suppressed by applying a magnetic field, the anomalous volume thermal expansion should disappear. We can see this effect in Fig. 6. The curves of volume thermal expansion at 0, 1, 5, and 12 T are plotted vs  $T$ . The anomalous effect is reduced as the field is greater, and at 12 T the volume thermal expansion curve is the anharmonic phonon contribution. The inset of Fig. 6 shows the extra contribution over the phonon contribution  $[\Delta V/V(H) - \Delta V/V(12T)]$  at  $H = 0, 1, \text{ and } 5$  T.

In Fig. 7 the  $\rho$  vs  $H$  isotherms below  $T_c$  are shown. The inset shows the isotherms above  $T_c$ . The shape of the curves below and above  $T_c$  is completely different. This reflects the fact that two different mechanisms are responsible for the magnetoresistance above and below  $T_c$ . Above  $T_c$  the high resistivity comes from the electronic localization. At  $T > T_c$  the effect of the magnetic field is to release the electrons which had become localized. The  $\rho$  vs  $T$  curves have a curvature which changes from negative to positive at a field ( $H_c$ ), which moves upwards with increasing temperatures.

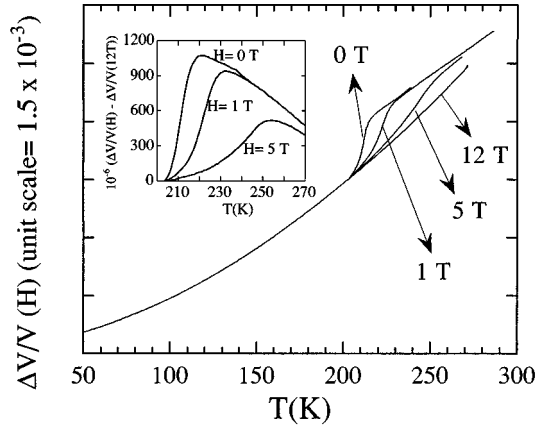


FIG. 6. Volume thermal expansion [ $\Delta V/V(H)$ ] under magnetic field values of 0, 1, 5, and 12 T. The inset shows the differences between the 0, 1, and 5 T curves and the 12 T curve.

Below  $H_c$  the resistivity is rather flat, evolving rapidly above  $H_c$  toward a tendency to saturation. As localization and strain are correlated in this compound, magnetostriction effects are expected above  $T_c$ . In Fig. 8(a) the volume magnetostriction isotherms are shown. They are extremely similar to the magnetoresistance isotherms. It seems clear that above  $T_c$  the charge localization and the local distortion which take place at zero field are released by applying a magnetic field, causing large magnetoresistance and volume magnetostriction effects. Below  $T_c$  the magnetoresistance comes mainly (as we have shown) from the spin alignment of the Mn spins by applying a magnetic field. The  $\rho$  vs  $H$  curves have a positive curvature and a rapid change of resistance takes place at low fields. Consequently, GMR is more useful below  $T_c$  because it takes place at low fields. Below  $T_c$  the volume magnetostriction is expected to be negligible. In Fig. 8(b) we can see the temperature dependence of the volume magnetostriction and the anisotropic magnetostriction at the maximum field, 14.2 T. The volume magnetostriction is large above  $T_c$  due to the correlation between localization and striction. At  $T_c$ , when the localization process is quenched, the volume magnetostriction rapidly vanishes.

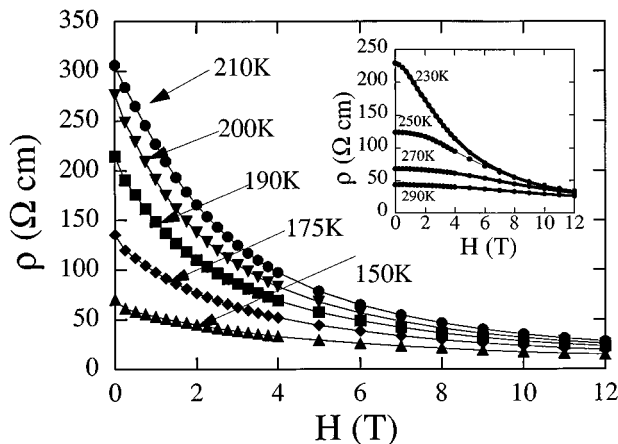


FIG. 7. Resistivity ( $\rho$ ) vs magnetic field at temperatures below  $T_c$ . The inset shows the same curves above  $T_c$ .

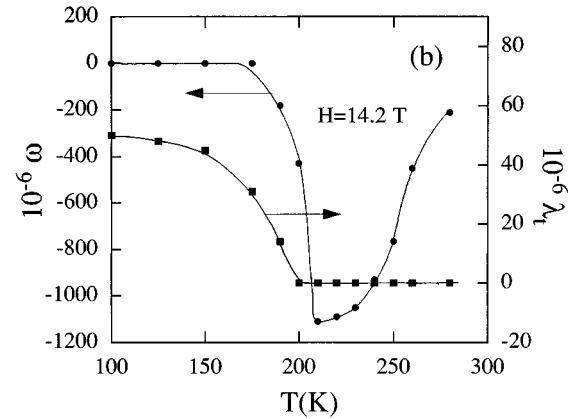
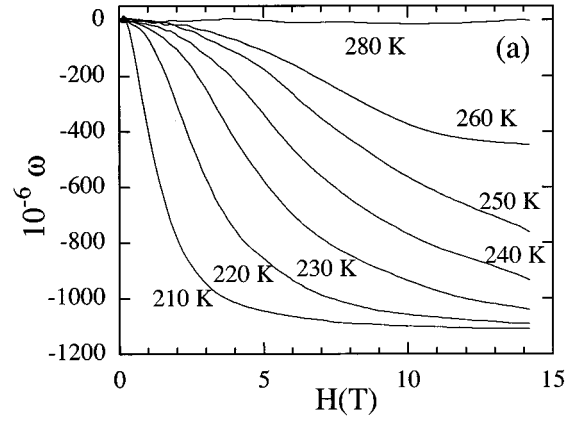


FIG. 8. (a) Volume magnetostriction ( $\omega$ ) vs magnetic field at temperatures above  $T_c$ . (b) Volume magnetostriction ( $\omega$ ) and anisotropic magnetostriction ( $\lambda_r$ ) as a function of temperature at  $H=14.2$  T.

The anisotropic magnetostriction is that typical of a ferromagnetic compound: zero above  $T_c$  and small below  $T_c$ .

### C. Effect of pressure

The effect of pressure on the properties of this compound is not obvious to predict. In Ref. 9 the authors suggest that the volume of the unit cell could be the important parameter to increase the resistivity. Hwang *et al.*<sup>12</sup> proposed a universal phase diagram, where  $T_c$  is diminished and the magnetoresistance is increased with increasing chemical pressure. From this phase diagram one could conclude that external pressure also should shift the insulator-metal transition toward lower  $T_c$  values and higher resistances. Measurements under pressure on  $\text{La}_{0.6}\text{Y}_{0.07}\text{Ca}_{0.33}\text{MnO}_3$ ,<sup>31</sup>  $\text{La}_{1-x}\text{Ca}_x\text{MnO}_3$ ,<sup>32</sup> and  $\text{La}_{1-x}\text{Sr}_x\text{MnO}_3$  (Ref. 33) have shown that external pressure shifts the transition toward higher temperatures and decreases the resistivity at all temperatures.

In Fig. 9 we can see the resistivity results under pressures of 0, 5, and 7 kbar. From the maxima of the curves  $dT_{\text{max}}/dP=2.2$  K/kbar. The resistivity decreases with pressure across the whole range of temperatures. In the inset of Fig. 9 we have plotted  $\ln \rho$  vs  $T^{-1/4}$  to check if conduction by magnetic polarons takes place under such pressures. The curves are linear, which suggests that up to 7.7 kbar the conduction is via magnetic polarons above  $T_c$ . How can one

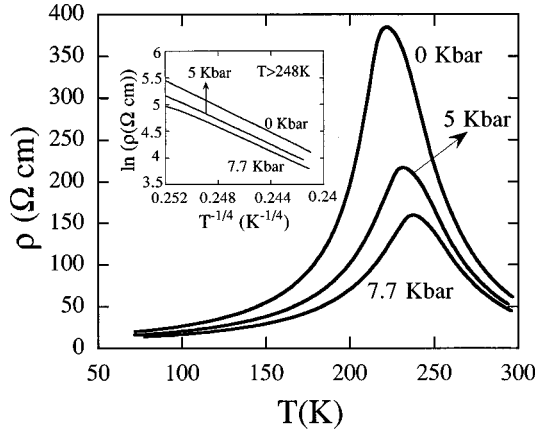


FIG. 9. Resistivity ( $\rho$ ) as a function of temperature under pressure values of 0, 5, and 7.7 kbar. The inset shows  $\ln \rho$  vs  $T^{-1/4}$  at temperatures above  $T_c$ .

explain this pressure dependence of  $T_c$ ? If  $T_c$  is increased by applying pressure, it is because the DE interaction, responsible for the ferromagnetism in this compound, is enhanced. The strength of the DE interaction is measured through the transfer integral between neighboring Mn sites,  $t_{\text{eff}} = t_0 \cos(\Theta/2)$ . As  $t_0$  depends on the length and angle of the Mn-O bond, it is expected to be strongly pressure dependent. It has recently been demonstrated by neutron crystallography under pressure<sup>34,35</sup> that in the perovskite  $\text{PrNiO}_3$  the main effect of external hydrostatic pressure is to reduce the cell volume, increasing the dense packing of the oxygen ions around the La/Ca ions. Consequently, the  $\text{NiO}_6$  octahedra are less tilted because there is less empty space around the La/Ca ions to fill. The same effect is expected to take place in  $\text{La}_{2/3}\text{Ca}_{1/3}\text{MnO}_3$ . By applying external pressure the Mn-O-Mn angle should increase toward  $180^\circ$  and the Mn-O bond length should decrease.<sup>36</sup> All this should increase  $t_0$  and consequently  $t_{\text{eff}}$ . The more effective transfer of the  $e_g$  electrons with pressure causes the resistivity to drop and  $T_c$  increase.

The low-temperature resistivity under pressure has also been fitted to the expression  $\rho(T) = \rho_0 + \rho_1 T^{2.5}$ . We show the fits in the inset of Fig. 10. In Fig. 10 we have plotted  $\rho_0$  and  $\rho_1$  vs  $P$  obtained from such fits. A linear relationship seems to exist up to 7.7 kbar. We can observe that the effect of the pressure differs from the effect of the field even though both of them diminish the resistivity. The pressure affects  $\rho_1$  more than  $\rho_0$ , whereas we have previously seen that the field affects  $\rho_0$  mainly. From the dependence of  $\rho_0$  and  $\rho_1$  with pressure, we can deduce that the pressure mainly decreases the temperature-dependent mechanisms of scattering: electron-electron, electron-magnon, and electron-phonon scattering. The temperature-independent mechanisms of scattering are also affected. Two factors are expected to be important. As we are measuring a polycrystalline sample, with nonzero porosity, the pressure should affect the connections between the grains just mechanically. The size of the magnetic domains can also be increased with pressure.

In Fig. 11 we can see the ac susceptibility and the volume thermal expansion under pressure. From the ac susceptibility we obtain the slope of the dependence of the temperature of the insulator-metal transition with pressure:  $dT_c/dP = 2.2$  K/kbar. The values of  $T_c$  obtained in the ac susceptibility

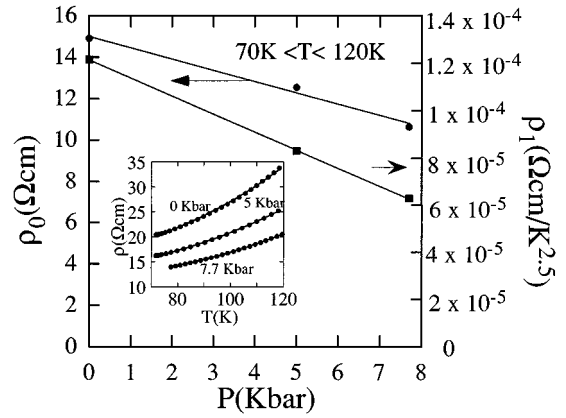


FIG. 10. Values of  $\rho_0$  and  $\rho_1$  obtained from the fits of the low-temperature resistivity to the expression  $\rho(T) = \rho_0 + \rho_1 T^{2.5}$  as a function of pressure. The inset shows the fits of the low-temperature resistivity at 0, 5, and 7.7 kbar to the expression  $\rho(T) = \rho_0 + \rho_1 T^{2.5}$ .

measurements for all the pressures coincide with the maxima of the resistivity curves. The volume anomaly bound to the insulator-metal transition is shifted by pressure in the same way as the electrical and the magnetic anomaly. Moreover, the volume change at  $T_c$  is reduced with increasing pressure. This is a consequence of the incomplete charge localization above  $T_c$  when pressure is applied. Then there is less charge to be delocalized at  $T_c$  and the drop diminishes.

#### IV. CONCLUSIONS

Microscopic and macroscopic techniques have been used to probe the anomalous spontaneous behavior of  $\text{La}_{2/3}\text{Ca}_{1/3}\text{MnO}_3$ . The experiments have shown that below  $T_p$  and above  $T_c$  there is a gradual charge localization which brings about local volume distortions and ferromagnetic clusters (short-range magnetic order). This supports the theory of conduction by magnetic polarons above  $T_c$ . At  $T_c$  an insulator-metal-like transition takes place and a volume anomaly ( $\approx 0.1\%$ ) appears. Above  $T_c$  the effect of the magnetic field and pressure is to increase the transfer integral of

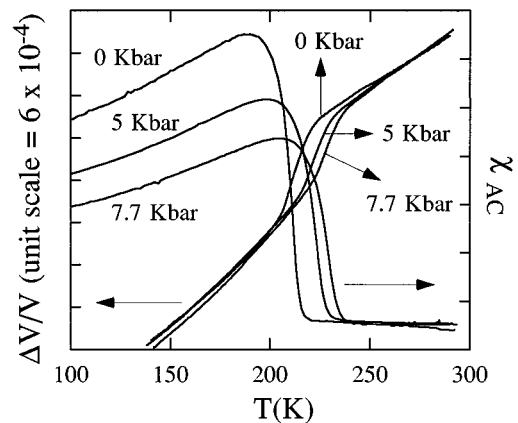


FIG. 11. ac susceptibility ( $\chi_{\text{ac}}$ ) and volume thermal expansion ( $\Delta V/V$ ) as a function of temperature at pressure values of 0, 5, and 7.7 kbar.

the  $e_g$  electrons between adjacent Mn ions, reducing the charge localization and favoring the metallic state. Consequently, the electrical and volume anomalies at  $T_c$  are strongly reduced. Below  $T_c$  two mechanisms are responsible for the resistivity: a temperature-independent scattering of the electrons (due to domain and grain boundaries, defects, etc.) and other temperature-dependent mechanisms (electron-electron, electron-phonon, and electron-magnon scattering). Low magnetic fields strongly reduce the scattering due to

domain boundaries giving rise to GMR at low fields. The pressure reduces more the temperature-dependent mechanisms.

#### ACKNOWLEDGMENTS

We acknowledge the financial support of the Spanish CICYT under Grants No. MAT-96-0826, No. MAT-96-0491, and No. APC-95-0123.

- 
- <sup>1</sup>G. H. Jonker and J. H. Van Santen, *Physica* **16**, 337 (1950); G. H. Jonker, *ibid.* **22**, 707 (1956).
- <sup>2</sup>C. Zener, *Phys. Rev.* **81**, 440 (1951); **82**, 403 (1955).
- <sup>3</sup>E. O. Wollan and W. C. Koehler, *Phys. Rev.* **100**, 545 (1955).
- <sup>4</sup>J. H. Van Santen and G. H. Jonker, *Physica* **16**, 599 (1950).
- <sup>5</sup>R. M. Kusters, J. Singleton, D. A. Keen, R. McGreevy, and W. Hayes, *Physica B* **155**, 362 (1989).
- <sup>6</sup>R. Von Helmolt, J. Wecker, B. Holzapfel, L. Schultz, and K. Samwer, *Phys. Rev. Lett.* **71**, 2331 (1993).
- <sup>7</sup>Ken-ichi Chahara, T. Ohno, M. Kasai, and Y. Kozono, *Appl. Phys. Lett.* **63**, 1990 (1993).
- <sup>8</sup>M. McCormack, S. Jin, T. H. Tiefel, R. M. Fleml, and Julia M. Phillips, *Appl. Phys. Lett.* **64**, 3045 (1994).
- <sup>9</sup>S. Jin, H. M. O'Bryan, T. H. Tiefel, M. McCormack, and W. W. Rhodes, *Appl. Phys. Lett.* **66**, 382 (1995).
- <sup>10</sup>A. Maignan, Ch. Simon, V. Caignaert, and B. Raveau, *Solid State Commun.* **96**, 623 (1995).
- <sup>11</sup>Guo-Qiang Gong, Chadwick Canedy, Gang Xiao, Jonhatan Z. Sun, Arunava Gupta, and William J. Gallagher, *Appl. Phys. Lett.* **67**, 1783 (1995).
- <sup>12</sup>H. Y. Hwang, S.-W. Cheong, P. G. Radaelli, M. Marezio, and B. Batlogg, *Phys. Rev. Lett.* **75**, 914 (1995).
- <sup>13</sup>A. Urushibara, Y. Moritomo, T. Arima, A. Asamitsu, G. Kido, and Y. Tokura, *Phys. Rev. B* **51**, 14 103 (1995).
- <sup>14</sup>A. J. Millis, P. B. Littlewood, and B. I. Shraiman, *Phys. Rev. Lett.* **74**, 5144 (1995).
- <sup>15</sup>K. Kubo and N. Ohata, *J. Phys. Soc. Jpn.* **33**, 21 (1972).
- <sup>16</sup>N. Furukawa, *J. Phys. Soc. Jpn.* **64**, 2754 (1995).
- <sup>17</sup>Fa-jian Shi, Meng Ding, and Tsung-han Lin, *Solid State Commun.* **96**, 931 (1995).
- <sup>18</sup>J. M. D. Coey, M. Viret, L. Ranno, and K. Ounadjela, *Phys. Rev. Lett.* **75**, 3910 (1995).
- <sup>19</sup>M. R. Ibarra, P. A. Algarabel, C. Marquina, J. Blasco, and J. García, *Phys. Rev. Lett.* **75**, 3541 (1995).
- <sup>20</sup>T. A. Tyson, J. Mustre de Leon, S. D. Conradson, A. R. Bishop, J. J. Neumeier, and Zang Jun (unpublished); P. Dai, Jiandi Zhang, H. A. Mook, S.-H. Liou, P. A. Dowben, and E. W. Plummer (unpublished).
- <sup>21</sup>J. S. Ramachandran, S. M. Bhagat, J. L. Peng, and M. Rubinstein, *Solid State Commun.* **96**, 127 (1995).
- <sup>22</sup>H. L. Ju, J. Gopalakrishnan, J. L. Peng, Qi, G. C. Xiong, T. Venkatesan, and R. L. Greene, *Phys. Rev. B* **51**, 6143 (1995).
- <sup>23</sup>G. C. Xiong, Q. Li, H. L. Ju, R. L. Greene, and T. Venkatesan, *Appl. Phys. Lett.* **66**, 1689 (1995).
- <sup>24</sup>P. Schiffer, A. P. Ramirez, W. Bao, and S.-W. Cheong, *Phys. Rev. Lett.* **75**, 3336 (1995).
- <sup>25</sup>J. Inoue and S. Maekawa, *Phys. Rev. Lett.* **74**, 3407 (1995); J. M. De Teresa, M. R. Ibarra, J. García, J. Blasco, C. Ritter, P. A. Algarabel, C. Marquina, and A. del Moral, *Phys. Rev. Lett.* **76**, 3392 (1996).
- <sup>26</sup>N. F. Mott, *Adv. Phys.* **21**, 785 (1972).
- <sup>27</sup>In Ref. 5 the authors report that in  $\text{Nd}_{0.5}\text{Pb}_{0.5}\text{MnO}_3$  they have observed diffuse scattering above  $T_c$ , consistent with dynamic fluctuations in the magnetic structure. They say that such fluctuations can be produced by the hopping of magnetic polarons.
- <sup>28</sup>L. Van Hove, *Phys. Rev.* **95**, 249 (1954); **95**, 1374 (1954).
- <sup>29</sup>M. K. Wilkinson and C. G. Shull, *Phys. Rev.* **103**, 516 (1956).
- <sup>30</sup>P.-G. de Gennes, *Phys. Rev.* **118**, 141 (1960).
- <sup>31</sup>Z. Arnold, K. Kamenev, M. R. Ibarra, P. A. Algarabel, C. Marquina, J. Blasco, and J. García, *Appl. Phys. Lett.* **67**, 2875 (1995).
- <sup>32</sup>J. J. Neumeier, M. F. Hundley, J. D. Thompson, and R. H. Heffner, *Phys. Rev. B* **52**, R7006 (1995).
- <sup>33</sup>Y. Moritomo, A. Asamitsu, and Y. Tokura, *Phys. Rev. B* **51**, 16 491 (1995).
- <sup>34</sup>P. Canfield, J. D. Thompson, S.-W. Cheong, and L. W. Rupp, *Phys. Rev. B* **47**, 12 357 (1993).
- <sup>35</sup>M. Medarde, J. Mesot, P. Lacorre, S. Rosenkranz, P. Fischer, and K. Gobrecht, *Phys. Rev. B* **52**, 9248 (1995).
- <sup>36</sup>H. Y. Hwang, T. T. M. Palstra, S.-W. Cheong, and B. Batlogg, *Phys. Rev. B* **52**, 15 046 (1995).